The present direction as set forth in claim 1 is directed to a photocatalytic powder comprising titanium dioxide fine particles comprising an anionically active substance, wherein the fine particles have an electrokinetic potential of from about -100 mV to -10 mV in an aqueous environment at pH 5, and wherein the titanium dioxide fine particles are obtained by a vapor phase reaction or a wet-hydrolyzing.

The present direction as set forth in claim 2 is directed to a photocatalytic powder comprising titanium dioxide fine particles comprising an anionically active substance, wherein the fine particles have an electrokinetic potential of from about -100 mV to -10 mV in an aqueous environment at pH 5, and wherein the crystal form of the titanium dioxide fine particles is anatase and/or brookite.

In the present invention, the titanium dioxide fine particles can be in any of the following states: the titanium dioxide fine particles contain an anionically active substance which is present in the vicinity of the surface of the fine particles, or an anionically active substance is adsorbed to the surface of a titanium dioxide fine particle, or an anionically active substance is present in the vicinity of the surface of titanium dioxide. See page 6, lines 13-17 of the present specification. This is why the fine particles of the present invention have an electrokinetic potential of from about -100mV to -10mV in an aqueous environment at a pH of 5.

Accordingly, the present invention provides a photocatalytic powder and a photocatalytic slurry, which can exhibit not only excellent photocatalytic activity and durability, but also dispersion stability when coated on the surface of fiber, paper or plastic material, kneaded into

such a material, or used for a coating composition. See page 3, lines 25-29 of the present specification.

On the other hand, Taoda et al '736 is directed to a photocatalytic powder comprised of finely divided titanium dioxide particles having a coating of porous calcium phosphate formed on at least part of the surface of each finely divided titanium dioxide particle, wherein an anionic surface active agent is present at least on the interface between the porous calcium phosphate coating and the finely divided titanium dioxide particle.

Taoda et al '736 is silent on the dispersion stability when the powder is coated on the surface of fiber, paper or plastic material, kneaded into such a material, or used for a coating composition. Taoda et al '736 only disclose that when the powder is supported on an organic polymer medium, the durability of the organic polymer medium is improved. See column 3, lines 4-11 of Taoda et al '736.

In Taoda et al '736, most of the anionic surface active agent must be present on the interface between the calcium phosphate and the finely divided titanium dioxide particle, because the anionic surface active agent improves the adhesive force of the porous calcium phosphate coating to the titanium dioxide particle. See column 4, lines 43-53 of Taoda et al '736.

Accordingly, Taoda et al '736 do not indicate a control of the electrokinetic potential on the fine particles. As a result, the dispersion stability can not be resolved.

From the above facts, it can be understood that the surface of the calcium phosphate coated fine particles in Taoda et al '736 is different from the surface of the fine particles of the present invention, because in the present invention most of the anionic active substance is present on the surface of the particles, whereas in Taoda et al '736 most of the anionic active substance must be present on the interface that exists between the calcium phosphate coating and the finely divided titanium dioxide particles, because the anionic surface active agent improves the adhesive force of the porous calcium phosphate coating to the titanium dioxide particle. See column 4, lines 43 to 53.

That is to say, the surface of the fine particle in Taoda et al '736 is comprised of calcium phosphate and titanium dioxide, and as a result the electrokinetic potential of the powder in Taoda et al '736 is outside of the claimed range in the present invention.

The Examiner acknowledges in the present Office Action that applicants have argued that the photocatalytic powder disclosed in Taoda et al is different from that of the present claims because the powder in Taoda et al contains a coating of porous calcium phosphate formed on at least part of the surface of each of the finely divided titanium oxide particles. The Examiner states that this argument is not persuasive because the "porous calcium phosphate" of Taoda et al is not excluded from the scope of the present claims since the present claims contain the open-ended phrase "comprising". The Examiner refers to claim 1, line 2.

In response, applicants point out that the porous calcium phosphate of Taoda et al affects the electrokinetic potential of the powders, and would cause the powders of Taoda et al to not have the electrokinetic potential recited in the present claims. The present claims implicitly

exclude components, structures and amounts which would cause the powders to not have the recited electrokinetic potential.

In support of applicants' position that the calcium phosphate in Taoda et al, which as disclosed at column 5, lines 33 to 37 is preferably hydroxyapatite, would cause the powders of Taoda et al to not have the electrokinetic potential recited in the present claims, applicants enclose herewith a copy of an article by Vasudevan et al, "Interaction of Pyrophosphates with Calcium Phosphates", *Langmuir*, Vol. 10, No. 1 (1994), pages 300 to 325. Figure 2 at page 321 shows that the electrokinetic potential of HAP (hydroxyapatite) at a pH of 5 is zero, which is outside the range of the present claims. Since the powders of Taoda et al contain calcium phosphate as a coating, applicants submit that one of ordinary skill in the art would expect that the powders of Taoda et al would not have the electrokinetic potential recited in the present claims.

Further, to the extent that the powders of Taoda et al contain titanium dioxide on their surface, this would not change the conclusion that one of ordinary skill in the art would expect that the powders of Taoda et al would not have the electrokinetic potential recited in the present claims. Applicants refer the Examiner to the following four documents in support of their position (copies of the first three documents are enclosed herewith):

(1) "Zeta Potential and Surface Charge Components at Anatase/Electrolyte Interface", *Journal of Colloid and Interface Science*, Vol. 110, No. 1, (1986), pages 278 to 281, which shows at page 279, Fig. 1, that the electrokinetic potential of titanium dioxide in an aqueous environment at pH 5 is more than zero.

(2) S. Lee et al, Journal of Membrane Science, Vol. 201 (2002), page 193, which discloses that the point of zero charge of titania (TiO_2) has a pH of 6.25.

(3) A University of Alabama publication which contains a Figure that shows a point of zero charge at a pH of 6 (see Curve A of the Figure) for titania (titanium dioxide);

(4) U.S. Patent 4,241,042 to Matijevic et al, was cited in the Information Disclosure Statement of December 2, 2003, and which discloses at column 7, lines 35 to 37, that the "particles of this invention [titanium dioxide] normally possess an electrokinetic point of zero charge at a pH in the range of from 4.0 to 5.5".

Applicants submit that from these disclosures, one of ordinary skill in the art would conclude that the electrokinetic potential of titanium dioxide in an aqueous environment at a pH of 5 is zero or higher, and not within the scope of the present claims.

From the above facts, applicants submit that one of ordinary skill in the art would conclude that the electrokinetic potential of the powders in Taoda et al is zero or more than zero, and does not satisfy the recitation of the present claims that the fine particles have electrokinetic potential from about -100mV to -10mV in an aqueous environment at pH 5.

Further, with respect to applicants' argument that Taoda et al do not indicate a control of the electrokinetic potential on the fine particles, the Examiner states that this argument is not persuasive because the Taoda et al particles are the same as those of the present claims and, therefore, would be expected to have the same characteristics, such as the claimed electrokinetic potential properties. The Examiner states that even though Taoda et al is silent with respect to the photocatalytic powder properties, Taoda et al inherently satisfy this recitation.

In response, as can be seen from the above discussion, applicants submit that the powders of Taoda et al are not the same as those of the present claims because the present claims implicity exclude components, structures and amounts would cause the powders to not have the recited electrokinetic potential, and that one of ordinary skill in the art would understand that the electrokinetic potential of the powders in Taoda et al would not satisfy the recitation of the present claims that the fine particles have and electrokinetic potential from about -100mV to -10mV in an aqueous environment at pH 5, especially since the powders of Taoda et al have calcium phosphate on their surface which affects the electrokinetic potential of the particles. Accordingly, the powders of Taoda et al would not inherently have the electrokinetic potential recited in the present claims.

In view of the above, applicants submit that Taoda et al '736 do not defeat the patentability of claims 1 to 19 and, accordingly, request withdrawal of this rejection.

Claim 19 has been rejected under 35 U.S.C. § 103(a) as obvious over Taoda et al '736 in view of Suzuki et al.

The Examiner states that Taoda et al '736 disclose a photocatalytic powder as described above except for the presence of activated carbon and/or zeolite. The Examiner relies on the Suzuki et al patent to supply the teachings of the use of activated carbon with titanium dioxide fine particles.

Claim 19 is a dependent claim that depends ultimately from claim 1 or 2. Accordingly, applicants submit that claim 19 is patentable for the reasons discussed above in connection with the rejection of claims 1 and/or 2.

In view of the above, reconsideration and allowance of this application are now believed to be in order, and such actions are hereby solicited. If any points remain in issue which the Examiner feels may be best resolved through a personal or telephone interview, the Examiner is kindly requested to contact the undersigned at the telephone number listed below.

The USPTO is directed and authorized to charge all required fees, except for the Issue Fee and the Publication Fee, to Deposit Account No. 19-4880. Please also credit any overpayments to said Deposit Account.

Respectfully submitted,

Sheldon I. Landsman

SUGHRUE MION, PLLC
Telephone: (202) 293-7060
Facsimile: (202) 293-7860

WASHINGTON OFFICE
23373
CUSTOMER NUMBER

Sheldon I. Landsman
Registration No. 25,430

Date: April 4, 2005

Langmuir 1994, *10*, 320–325

Interaction of Pyrophosphate with Calcium Phosphates

T. V. Vasudevan† and P. Somasundaran

Langmuir Center for Colloids and Interfaces, Columbia University, New York, New York 10027

C. L. Howie-Meyers, D. L. Elliott,‡ and K. P. Ananthapadmanabhan*

Unilever Research, Edgewater, New Jersey 07020

Received April 22, 1993. In Final Form: October 25, 1993®

Interactions of pyrophosphate (PP) with hydroxyapatite (HAP), brushite, and calcium pyrophosphate (CaPP) have been studied using electrokinetic and ESCA measurements. PP adsorbs on HAP and brushite even when their surfaces are highly negatively charged. Importantly, the HAP zeta potential curves as a function of PP concentration show a precipitous drop in the low concentration range. Also, curves at different pH values show a progressive shift in the potential toward that of CaPP. These observations suggest the formation of CaPP on HAP surface and this has been further confirmed by ESCA studies. Thus, adsorption on HAP appears to involve a surface precipitation or chemisorption followed by surface precipitation or surface reaction phenomenon. It is also suggested that in the case of brushite the dissolved calcium from the mineral competes for the PP and in turn reduces its adsorption.

Introduction

Regulation of calcium phosphate crystal growth is important in a wide variety of applications such as in the prevention of scale formation in industrial heat exchangers, in the removal of phosphates from polluted water, and, most importantly, in the biological mineralization of teeth and bones.[1-5] Pyrophosphates (PP) are known to inhibit formation and growth of calcium phosphate precipitates. Reported studies[6-10] show that the inhibitory activity of PP is due to its ability to adsorb on the growing nuclei and in turn block the crystal growth sites. In this regard, the adsorption of PP on hydroxyapatite (HAP) has been conducted and correlated with the crystal growth inhibition behavior in the past;[6-10] however, the mechanism of adsorption itself has not been fully established. Also, interaction of PP with brushite and other forms of calcium phosphate which exist as precursors to HAP during the formation of dental tartar[11] have not been examined. Significantly, while PP is an excellent inhibitor of HAP formation, it is only a moderate inhibitor of brushite crystal growth.[12]

In the present investigation, the interaction of PP with HAP and brushite has been studied using electrokinetic and X-ray photoelectron spectroscopic (ESCA) techniques. These techniques measure the changes in the interfacial properties, namely of charge and surface chemical composition of the substrate and, therefore, can provide insight into the mechanism of adsorption of PP on HAP and brushite.

Experimental Section

Materials. *Calcium Phosphates.* HAP and brushite powders were obtained from Albright and Wilson. The surface areas of these samples have been reported to be 26 and 3 m^2/g, respectively, as measured by the BET nitrogen adsorption technique. Calcium pyrophosphate (CaPP) was purchased from Alfa Products and used without further purification.

Pyrophosphate. Reagent grade tetrapotassium pyrophosphate (TKPP) was purchased from Sigma Chemical Co.

Other Reagents. Sodium hydroxide and hydrochloric acid, used as pH modifiers, and sodium chloride, used for adjusting the ionic strength, were supplied by Fisher Scientific Co. Triply distilled water was used for preparing the solutions and the suspensions.

Methods. *Zeta Potential Measurements.* Samples of solids (0.05 g) were added to 50 mL of 2×10^{-3} kmol/m^3 NaCl solution, of preadjusted pH, in a 150-mL beaker. The suspension was stirred for 2 h using a magnetic bar and the pH was measured at the end. Following this, 50 mL of 2×10^{-3} kmol/m^3 NaCl solution containing the desired concentration of TKPP was added to the suspension. Prior to addition, the pH of the TKPP solution was adjusted to that of the suspension. The solids were conditioned for 1 h with TKPP. At the end of the conditioning period, the pH of the suspension was measured and about 50 mL of the suspension was transferred to the cell of the zeta meter (Zeta Meter, Zeta Meter Inc.). The mobilities of 10 to 15 particles were measured and zeta potential was calculated. A chart provided with the zeta meter manual was used for the conversion of mobility readings to zeta potential values.

Calcium Binding Isotherms. One-milliliter samples of 10 wt % TKPP solution were added to 99 mL of solutions of varying calcium chloride concentration. The pH of the resulting suspension was adjusted to the desired value (pH 7.5 or pH 11.0) and the calcium activity measured using a pH meter equipped with an Orion Model 93-20 calcium selective electrode.

XPS Analysis. X-ray photoelectron spectroscopic analysis of the HAP, brushite, and CaPP samples was carried out at Physical Electronics Laboratories, Edison, NJ, using a Perkin-Elmer Model 5000LS ESCA spectrophotometer. Samples for XPS analysis were prepared by treatment of HAP and brushite powders with 200, 500, and 1000 ppm of TKPP in aqueous

† Present address: Unilever Research.

‡ Present address: Calgon Corp.

® Abstract published in *Advance ACS Abstracts,* December 15, 1993.

(1) Zuhl, R.; Amjad, Z.; Masler, W. F. *J. Cool. Tower Inst.* 1987, *8*, 41.
(2) Ferguson, J. F.; Jenkins, D.; Eastman, J. *J. Water Pollut. Control Fed.* 1973, *45*, 620.
(3) Nancollas, G. H. *Biological Mineralization and Demineralization*; Nancollas, G. H., Ed.; Springer Verlag: Berlin, 1982; p 79.
(4) Posner, A. S.; Blumenthal, N. C.; Betts, F. Chemistry and Structure of Hydroxyapatites. *Phosphate Minerals*; Nriagu, J. O., Moore, P. B., Eds.; Springer Verlag: Berlin, 1984, Chapter 11, pp 330–350.
(5) Salimi, M. H.; Heughebaert, J. C.; Nancollas, G. H. *Langmuir* 1985, *1*, 119.
(6) Fleisch, H.; Russel, R. G. G.; Straumann, F. *Nature* 1966, *212*, 901–903.
(7) Krane, S. M.; Glimcher, M. J. *J. Biol. Chem.* 1962, *237*, 2991–2998.
(8) Burton, F. G.; Neuman, M. W.; Neuman, W. F. *Curr. Mod. Biol.* 1969, *3*, 20–26.
(9) Jung, A.; Bisaz, S.; Fleisch, H. *Calcif. Tissue Res.* 1973, *11*, 269–280.
(10) Moreno, E. C.; Aoba, T.; Margolis, H. C. *Compend. Contin. Educ. Dent. Suppl.* 1987, *No. 8*, S253–S266.
(11) Schroeder, H. E.; et al. *Formation and Inhibition of Dental Calculus*; Hans-Huber: Vienna, 1969; pp 109–121.
(12) Elliott, et al., submitted for publication in *Arch. Oral Biol.*

0743-7463/94/2410-0320$04.50/0

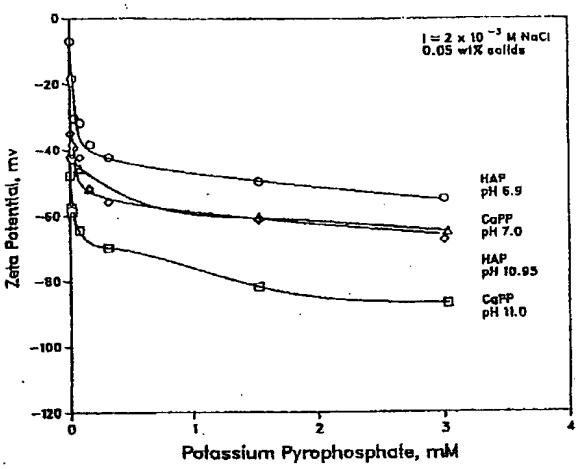

Figure 1. Zeta potential of HAP treated with pyrophosphate, effect of pH.

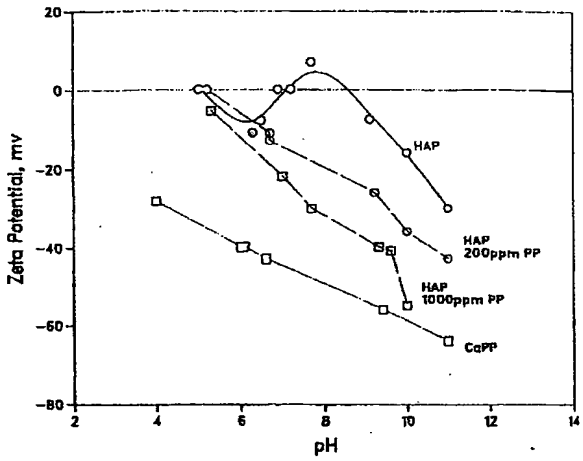

Figure 2. Effect of PP treatment on zeta potential of hydroxyapatite.

solution, followed by centrifugation and drying to yield fine powdered solids.

Results and Discussion

Interaction of Pyrophosphate with HAP. *Zeta Potential.* The zeta potential behavior of HAP was determined as a function of PP concentration at two different pH values and the results are shown in Figure 1. For comparison, the zeta potential of CaPP is also plotted in the same figure. In the absence of PP, HAP under both the tested pH conditions exhibits a negative charge. Interestingly, the potential at low levels of PP exhibits a precipitous drop to values close to that of CaPP. Beyond this concentration, the dependence of HAP potential on PP concentration becomes similar to that of CaPP. Note that the behavior is essentially the same at both pH values (7 and 11). The sharp reduction in the potential of HAP at low levels of PP, even under conditions when the HAP surface is highly negatively charged as at pH 11, clearly shows the strong affinity of PP for the surface. This behavior is indicative of an adsorption process involving a phase change, possibly the formation of CaPP on HAP surface. The observation that the potential of CaPP itself depends on PP concentration in solution is not surprising since the latter is a potential determining ion for the surface.

Note that beyond the precipitous drop in zeta potential of HAP in PP solutions, values of the potential are not identical to those of CaPP but vary similarly to that of CaPP. Even if PP forms a CaPP layer on HAP surface, differences between the potentials of CaPP and PP-treated HAP are not unreasonable. For example, PP, being a potential determining ion for CaPP, can lower the CaPP potential. Therefore, identical values of zeta potential of CaPP and PP-treated HAP can be expected if and only if the residual levels of all ionic species are the same in both the systems. Inhomogeneties in the newly formed CaPP layer on HAP can also cause differences between the potentials of CaPP and PP-treated HAP.

The pH dependence of the zeta potential of HAP treated with solutions containing different levels of PP is shown in Figure 2. Again for comparison, the zeta potential of CaPP is included. It is evident from the zeta potential curves that the surface of HAP is becoming more negative with increase in PP concentration. Also, the curves appear to progressively shift toward that of CaPP. While this in itself cannot be taken as evidence of CaPP formation, this in combination with the data in Figure 1 suggests the formation of CaPP on HAP surface.

Formation of CaPP on HAP can occur by either a surface precipitation phenomenon or a surface reaction process. Surface reaction involves chemical interaction between the adsorbate species and the adsorbent, in this case pyrophosphate and the HAP surface. The reaction begins at the interface and proceeds inward. Surface precipitation, on the other hand, is the nucleation and growth of a stoichiometric precipitate of the adsorbate species by a complexing ion at the interface. In the present case, it will be the precipitation of CaPP on HAP surface. Note that often prior to surface precipitation, chemisorption of the adsorbate species can occur at the interface. Chemisorption can be distinguished from surface precipitation in the following manner. Chemisorption usually refers to adsorption resulting from the formation of a high-energy bond, such as a covalent bond, between the adsorbate species and site/sites on the solid surface and this will not result in the formation of a stoichiometric compound. Note that chemisorption can occur even if electrostatic factors are unfavorable for adsorption.

Adsorption has been shown to involve surface reaction or surface precipitation in a number of other mineral/inorganic systems in the past.[13,14] For example, formation of calcium carbonate and calcium fluorite on a HAP surface in the presence of dissolved carbonate[13] and fluoride, respectively,[14] and formation of calcium phosphate on calcite in the presence of phosphate[13] have been shown to involve a surface reaction or surface precipitation phenomenon.

The results from the current study suggest that in the presence of PP formation of CaPP can occur on the HAP surface. In order to test whether this observation is consistent with the expected thermodynamic behavior of the system, the following analysis was conducted. Essentially the feasibility of the reaction:

$$6H^+ + Ca_{10}(PO_4)_6(OH)_2(s) + 5P_2O_7^{4-} \rightarrow 5Ca_2P_2O_7(s) + 6HPO_4^{2-} + 2OH^- \quad (1)$$

was examined using the literature values of free energy of formation of various species. The standard free energy

(13) Somasundaran, P.; Amankonah, J. O.; Ananthapadmanabhan, K. P. *Colloids Surf.* 1985, *15*, 309–333.
(14) Chander, S.; Fuerstenau, D. W. *Colloids Surf.* 1985, *13*, 137–144. Lin, J.; Raghavan, S.; Fuerstenau, D. W. *Colloids Surf.* 1981, *3*, 357–370.

Table 1. Free Energy of Formation for Reaction of HAP and PP

species	free energy of formation from elements, $G°_f$, kcal/mol	ref
H^+	0	
$Ca_{10}(PO_4)_6(OH)_2$(s)	−3030	15
HPO_4^{2-}	−260.3	15
$P_2O_7^{4-}$	−458.7	15
OH^-	−37.6	15
Ca^{2+}	−132.3	15
CaPP(s)	−748.6	15
	−743.6	16
	−741.95	17

Table 2. Calculation of PP Levels Required To Form CaPP

free energy of formation of $Ca_2P_2O_7$, kcal/mol	$\Delta G°$, kcal/mol	log K_{eq}	$[P_2O_7^{4-}]$, mol/L	$K_4P_2O_7$, ppm
−748.6	−56.7	41.7	3.2×10^{-10}	0.0002
−743.6	−31.6	23.2	1.6×10^{-6}	1.1
−741.95	−23.43	17.23	2.5×10^{-5}	16.5

change accompanying the reaction can be estimated from the free energies of formation of the reactants and products. The standard free energy change ($\Delta G°$) can be related to the equilibrium constant for the reaction, K, as

$$K = [HPO_4^{2-}]^6[OH^-]^2/[H^+]^6[P_2O_7^{4-}]^5 \quad (2)$$

Thus, if HAP is in equilibrium with the solution at a given pH (i.e. H^+, OH^-, and HPO_4^{2-} are fixed), then the minimum amount of $P_2O_7^{4-}$ required to force the above reaction to the right can be estimated.

The values of free energy of formation of various species and the source of the data are given in Table 1. As can be seen from the information in Table 1, there appears to be some uncertainty with regard to the value of free energy of formation of CaPP. The first value (−748.6 kcal/mol) was obtained from ref 15. The latter two values were obtained from unpublished work at Unilever Research.[16,17] The values −743.6 and −741.95 kcal/mol correspond to CaPP solubility product values of 1.2×10^{-15} and 1.9×10^{-14}, respectively. Since it was difficult to assess the accuracy of these estimates, each value was used to determine the corresponding three free energy and equilibrium constants for the above reaction. The results of this analysis are given in Table 2. The last two columns in the table show the concentrations of PP and TKPP for the present system at a pH of 6.9.

Note that because of pH-dependent hydrolysis reactions, only about 50% of the total PP will be $P_2O_7^{4-}$ at pH 6.9. This has been accounted for in the calculation of the concentration of TKPP in equilibrium with both of the solid phases. It is clear from Table 2 that from the three possible estimates of PP levels, the worst case situation, i.e., the highest concentration of TKPP needed to cause the formation of CaPP on HAP, is just above 16.5 ppm. This simple analysis indicates that the formation of CaPP on HAP in the presence of soluble PP at relatively low levels is consistent with the expected behavior, i.e., PP can replace orthophosphate on the mineral surface.

X-ray Photoelectron Spectroscopic Analysis (XPS/ESCA). In order to further confirm the formation of CaPP on the HAP surface in the presence of dissolved PP, an ESCA study was conducted. The XPS spectra of HAP, CaPP, and PP-treated HAP are shown in Figure 3. Figure

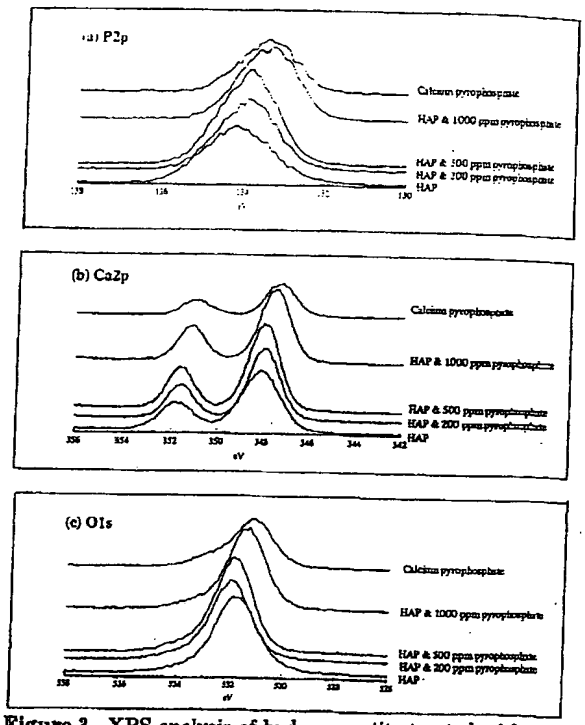

Figure 3. XPS analysis of hydroxyapatite treated with pyrophosphate.

3 is divided into parts a, b, and c which represent the binding energies corresponding to P2p (132–134 eV), Ca2p (347–348 eV), and O1s (531–532 eV), respectively. The XPS spectra for each element shows the spectra of untreated HAP, CaPP, and PP-treated HAP at PP concentrations of 200, 500, and 1000 ppm. For each element, the PP-treated HAP samples are between those of HAP and CaPP. The binding energy moves closer to CaPP as the concentration of TKPP increases. This indicates that the HAP surface, upon PP treatment, is becoming progressively similar to that of CaPP. Results of the XPS analysis thus support the inference, deduced from electrokinetic studies and thermodynamic analysis, of CaPP formation at the HAP surface.

Interaction of Pyrophosphate with Brushite. As in the case of HAP, the interaction of PP with brushite was also studied using zeta potential and ESCA techniques. The zeta potentials of brushite as a function of PP concentration are given in Figure 4. Here again, brushite is negatively charged under the test conditions and it shows a sharp reduction in potential after exposure to low levels of PP. Interestingly, the absolute values of the potential are lower than those observed for HAP. Also, beyond this initial drop there appears to be less dependence on PP concentration, in contrast to the behavior of the HAP/PP system described above. Thus, while zeta potential suggests some significant adsorption of PP on brushite, whether it involves surface conversion to a CaPP-type surface is not clear.

ESCA studies of brushite samples treated with PP were also conducted. Unlike the case of HAP, brushite and CaPP have very similar spectra and therefore it is not possible to use this technique to distinguish between the two phases.

One of the differences between HAP and brushite is their water solubility, with HAP having a relatively low solubility compared to brushite. For example, at a pH of

(15) *Lange's Handbook of Chemistry*; Dean, J. A., Ed.; Formerly compiled by Lange, N. A.; McGraw-Hill: New York, 1985.
(16) Welch, G. J.; Woosey, S. Unpublished results, Unilever Research, Port Sunlight, 1975.
(17) Clarke, D. E.; Lee, R. S.; Lunt, T. J. Unpublished results, Unilever Research, Port Sunlight, 1974.

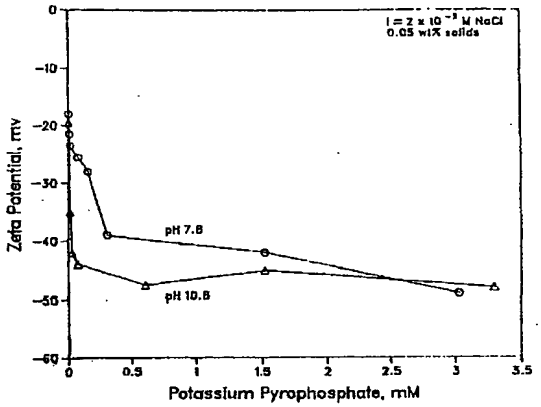

Figure 4. Zeta potential of brushite treated with pyrophosphate, effect of pH.

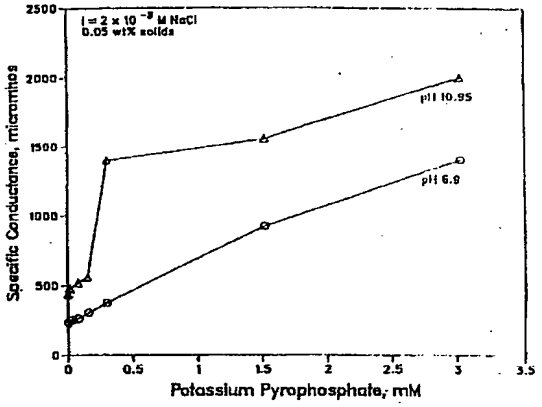

Figure 5. Specific conductance of HAP slurry in pyrophosphate solutions.

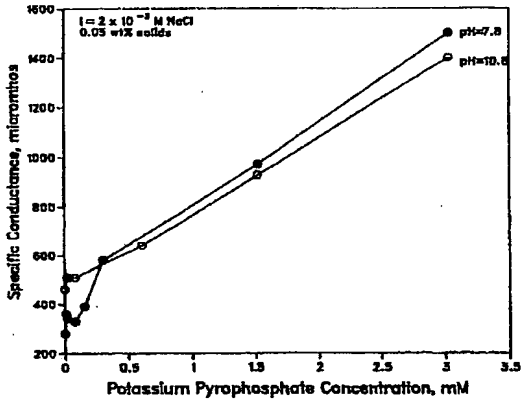

Figure 6. Specific conductance of brushite slurry in PP solutions.

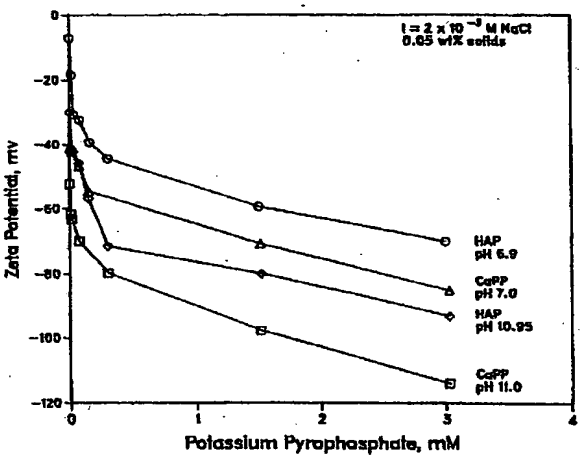

Figure 7. Zeta potential vs pyrophosphate concentration, zeta values corrected for ionic strength in PP solutions.

6.9, the concentration of calcium ions in equilibrium with HAP is about 2 ppm and that with brushite is about 28 ppm. When a reagent such as PP is introduced into a suspension of HAP or brushite, there exists a competition between complexation of bulk calcium vs adsorption. Because of the higher solution levels of calcium in the brushite suspensions, it is reasonable to expect that there will be more bulk complexation than in the case of HAP. This is supported by the observation that addition of 10 ppm of PP into supernatant solutions of HAP and brushite resulted in precipitation in the case of the latter and not in the case of the former. Thus, at a particular level of PP, there will be more PP available for surface adsorption/conversion on the HAP surface than on brushite. This may account for the differences in the dependence of zeta potential of HAP and brushite on PP concentration. This solubility difference appears to provide favorable conditions for bulk precipitation of CaPP in the brushite–PP system. In contrast to this, because of low calcium levels in solution, the interactions with HAP may be more like surface conversion or surface precipitation and this is in line with the ESCA results.

Comparison of Affinities of PP to HAP, Brushite, and CaPP. Zeta potential results presented in Figures 1 and 4 showed that addition of PP renders the surface of HAP and brushite negative. Therefore, variation of the charge density at the solid/liquid interface can be used as a measure of adsorption. Zeta potential values can be used as a measure of charge density at the solid/liquid interface and can be used for comparison provided the ionic strength of the medium is maintained constant since only the zeta potential, and not the charge density, depends on the ionic strength. As shown in Figures 5 and 6, addition of TKPP resulted in a significant increase of ionic strength, measured in terms of specific conductance. Therefore, the zeta potential results shown in Figures 1 and 2 were corrected for ionic strength variation using the procedure described by Hunter.[18]

Figures 7 and 8 show the zeta potential curves of TKPP-treated HAP and brushite corrected for a base ionic strength of 2×10^{-3} kmol/m^3 NaCl. Zeta potential curves obtained for the CaPP–TKPP system are presented in Figure 7 for the purpose of comparison. These corrected potentials can now be used to examine the dependence of zeta potential on pyrophosphate concentration. The approach involved the use of curve fitting software (Table Curve, Jandel Scientific, CA) to fit the experimental data to different forms of empirical equations. The equation that showed best fit (highest correlation coefficient) of the experimental data was obtained and is shown in Table 3. This empirical equation shows that the negative zeta potential of all three surfaces increases as a function of the square root of the PP concentration. In the equations shown in Table 3, the constant A represents the zeta potential of the untreated calcium phosphate, while B can be taken as a measure of the affinity of TKPP to the calcium phosphate surface. Examination of Table 3 shows

(18) Hunter, R. J. *Zeta Potential in Colloid Science: Principles and Applications*; Academic Press: New York, 1981; Chapter 2, pp 11–58.

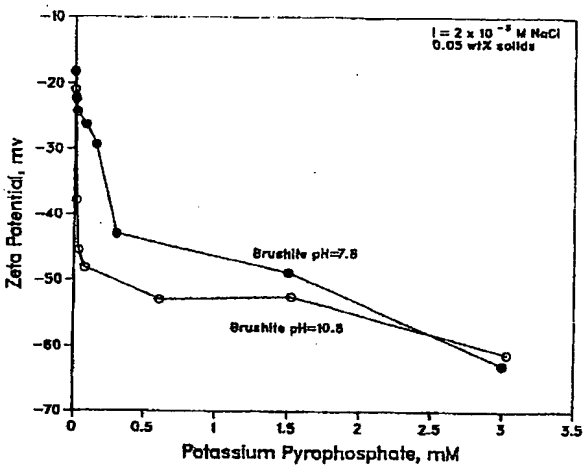

Figure 8. Zeta potential vs pyrophosphate concentration, zeta values corrected for ionic strength in PP solutions.

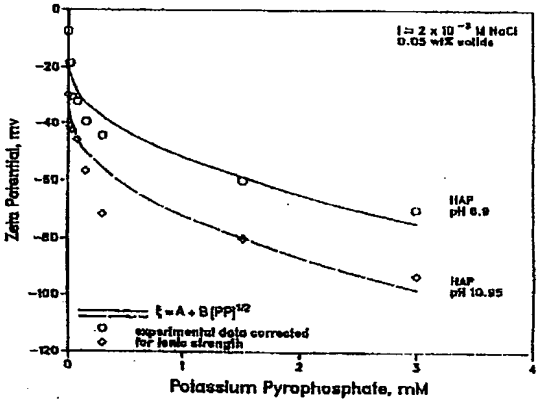

Figure 9. Zeta potential of HAP vs pyrophosphate concentration.

Table 3. Relationship Between Zeta Potential and Pyrophosphate Concentration: Empirical Models

Equation: $\xi = A + B\,[PP]^{1/2}$

	pH	A	B	ξ_{avg}	corr coeff
hydroxyapatite	6.90	−20.5	−31.4	−13.5	0.88
	10.95	−36.0	−36.0	−30.5	0.89
brushite	7.8	−20.6	−24.8	−18.3	0.94
	10.8	−31.9	−19.0	−21.0	0.62
calcium pyrophosphate	7.0	−41.0	−24.9	−41.4	0.98
	11.0	−57.4	−33.5	−52.3	0.99

that in all cases, except for the brushite–TKPP system at pH 11, the equation that best fitted the experimental data was of the same type in which the zeta potential showed a square root dependence on TKPP concentration. The quality of fit can be seen from Figures 9, 10, and 11 to be good for HAP and CaPP. Also, it can be seen from the "B" value that the affinity of TKPP is highest for HAP followed by CaPP and brushite. Further, the affinity of TKPP to the calcium phosphate surface is greater at higher pH. This is possibly due to differences in reactivity of $P_2O_7^{4-}$ present at high pH values vs $HP_2O_7^{3-}$ and other forms at lower pH.

Dissolved Calcium in the Supernatant of Calcium Phosphate Suspensions. Review of past results[10] and the results obtained in the present study suggest that the adsorption of PP on calcium phosphates involves chemical interactions and ultimately results from the formation of CaPP on HAP surface. Because of dissolution, the

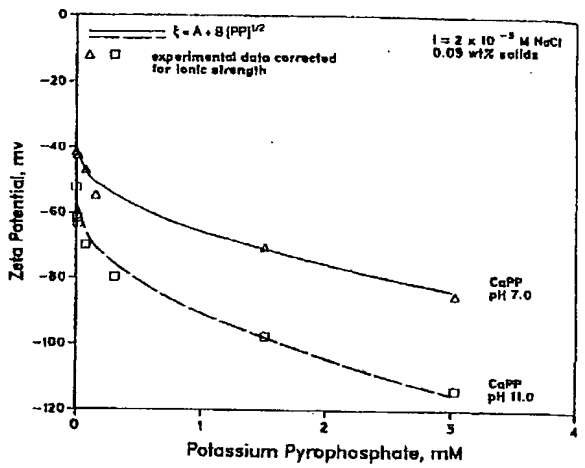

Figure 10. Zeta potential of CaPP vs pyrophosphate concentration.

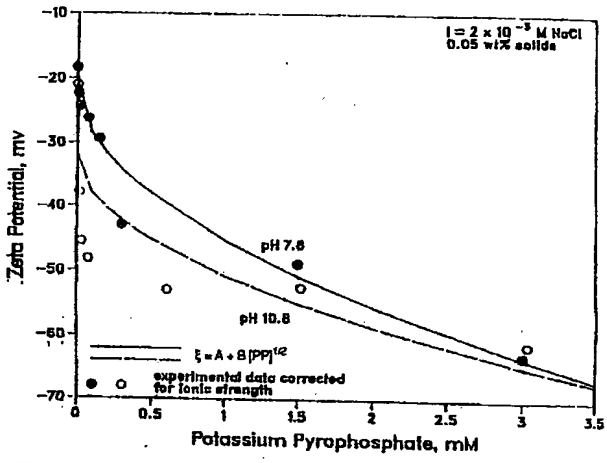

Figure 11. Zeta potential of brushite vs pyrophosphate concentration.

Table 4. Solubility of Calcium Phosphates

	pH	Ca^{2+}, ppm
hydroxyapatite	7.50	0.93
	10.74	<0.10
brushite	7.50	24.00
	10.85	1.50
calcium pyrophosphate	7.55	0.82
	10.80	<0.10

supernatant of calcium phosphate suspensions would contain calcium ions which would compete with the surface for PP molecules. The affinity of PP to calcium phosphate surface would thus depend on both the concentration of dissolved calcium and its relative affinity to the surface.

Table 4 shows the dissolved calcium concentration in the supernatants of HAP, brushite, and CaPP at pH values of 7.5 and 11. It can be seen that the dissolved calcium concentration is much higher at the lower pH for all three minerals. The dissolved calcium is much higher in brushite supernatant. Presence of larger levels of dissolved calcium can account for the lower affinity of PP to calcium phosphate surface at lower pH and also its lower affinity to brushite surface compared to that for HAP and CaPP. The dissolved calcium concentration in CaPP supernatant is similar to that of HAP supernatant. However, the affinity of TKPP is higher for HAP than for CaPP (Table 3). This is explained by comparing the electrostatic

repulsion at the two surfaces, where the repulsion between the negatively charged phosphate species and the surface would be higher for CaPP than for HAP, as evidenced by the much higher negative charge density of the CaPP surface (ZP = −41 mV) compared to that of HAP (ZP = −13.5 mV).

Conclusions

(1) Electrokinetic studies showed the negative zeta potential of HAP and brushite to increase sharply in the presence of very low concentrations of PP indicating strong affinity of the solute to the surface.

(2) Adsorption of negatively-charged PP species on highly negatively charged surfaces suggested chemisorption of solute on the surface. PP increased the negative potential of CaPP at pH 6.9 and 10.95, indicating that it is a potential-determining species for the surface.

(3) Formation of CaPP on the HAP surface was supported by the results from XPS and electrokinetic studies.

(4) Affinities of PP for HAP are found to be higher than that for brushite. Lower affinity for brushite was attributed to the presence of dissolved calcium in the supernatant which competes with surface calcium for PP.

(5) An empirical fit of the zeta potential data shows that the negative potentials on HAP, CaPP, and brushite increase as a function of the square root of the PP concentration. Greater affinity between PP and the surface was observed for both HAP and CaPP at the higher pH (~11) than at the lower pH (~7).

concentration (less than 500 μg/l of total organic carbon (TOC)) was prepared through a series of processes, which included two mixed beds of anion/cation exchange resins, an activated carbon cartridge, and a reverse osmosis membrane filter. TOC was measured using the UV/oxidants oxidation method (Dohrman, DC-180, US) with a TOC analyzer and an autosampler.

Nakdong river surface water (NR-SW) was sampled from the Bansong water treatment plant located at Changwon city (Korea), and immediately filtered through a 0.45 μm filter and stored in a refrigerator at 5 °C. Dissolved organic carbon (DOC) was measured, and NOM in NR-SW was separated into three different fractions: hydrophobic NOM, transphilic NOM, and hydrophilic NOM using the XAD-8 and XAD-4 isolation method [8,9]. Hydrophobic and transphilic NOM were mainly comprised of hydrophobic and hydrophilic acids, respectively [10]. Each fraction of the three NOM components were characterized by mass measurements, and the carboxylic and phenolic acidities of the hydrophobic and hydrophilic acids were determined using a micro-titrator (Metrohm, CH-910). Fifty milliliters samples were taken and acidified with 5N HCl (pH < 3.0), and sparged with nitrogen gas for at least 15 min to remove inorganic carbonate species. Incremental volumes of 2.0–25.0 μl of 0.05N NaOH were then added by micro-titrator to increase the pH to 10.0. The amount of 0.05N NaOH added allowed the determination of carboxylic (pH 3–8) and phenolic acidities (twice the amount between pH 8–10) [11]. The charge density of the NOM acids, as determined by the titration method, can be employed to demonstrate charge interactions between charged NOM acids and a negatively-charged membrane.

2.2. Membrane materials

Two different polymeric and four different ceramic membranes were used for PSD determinations. The nominal MWCOs used for each membrane were as stated by the manufacturers. We also determined the nominal MWCO of the membranes using PEG rejection tests and the resulting fractional rejections; the nominal MWCO of the membrane may be defined as the relative molecular mass of the component that is rejected by 90%. The fractional rejection of the PEG solute by the membrane was calculated using the following equation [12]:

$$R_{M_i} = \frac{W_{M_i}(\text{feed}) - W_{M_i}(\text{perm})(1 - R_{\text{overall}})}{W_{M_i}(\text{feed})} \quad (1)$$

where R_{M_i} is the fractional rejection of a certain RMM "i". W_{M_i} is the mass fraction of that RMM in the specific stream and R_{overall} is the overall amount of solute rejected by the membrane, based on DOC measurements.

The membrane surface charge was measured using zeta potential measurement and ionizable functional groups analysis. Zeta potential measurements of polymer membranes were performed by an electrophoretic method using a commercial instrument (ELS-8000, Otsuka Electronics, Japan) with a latex solution. The zeta potential was correlated with electrical mobility as measured by laser light scattering. Titania (TiO_2), the material that the ceramic membranes were composed of, has a point of zero charge (pH_{pzc}) of 6.25 [13]. We also measured the zeta potential values at various pH levels (4–8) to determine the iso-electric point (i.e.p.) of the ceramic membrane, with ground fine particles from a tubular type of ceramic membrane.

The charge density of the membrane surface can also be measured using a potentiometric titration, similar to the method used for NOM acidity measurement, as described. The active layer of the polymeric membrane sample (surface area = 58.9 cm^2) was cut into many small pieces, which were then placed in a titration vessel and potentiometrically titrated versus 0.05N NaOH to determine the presence of ionizable functional groups, quantitatively. The ceramic membrane was ground into fine particles, and the fine particles were put into a titration vessel for the potentiometric titration. Membrane charge density was calculated from the amount of 0.05N NaOH added, the units of functionality at a certain pH are expressed as milli-equivalents per gram dried membrane. The characteristics of membranes tested are shown in Table 1.

2.3. Membrane filtration apparatus and operation

The membrane filtration unit accommodated active filtration areas of 60.0 and 95.2 cm^2 for polymeric and ceramic membranes, respectively, and consisted of a membrane holder, pump with gear type pump head, needle valves (for the feed, retentate, and permeate streams), and pressure and flow-rate gauges. A

Zeta Potential of Titania Dispersion

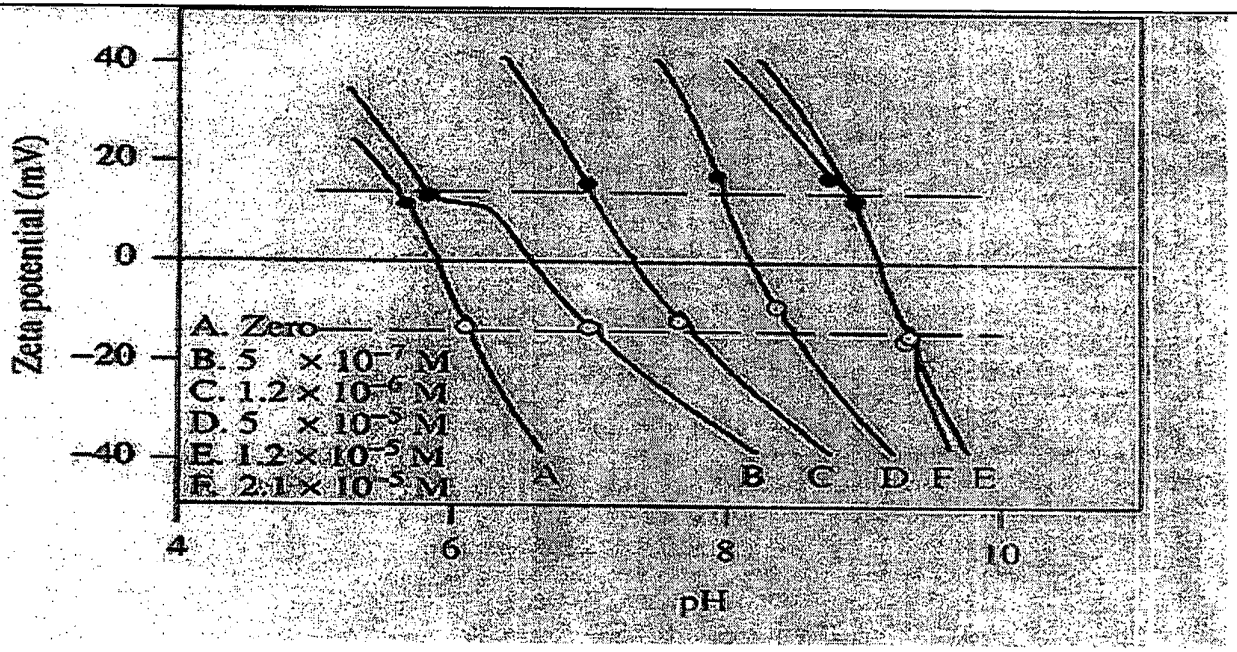

← Please see Sample A

The zeta potential of titania dispersion as a function of pH and concentration of aluminum nitrate.

R. O. James *et al. J. Coll. Int. Sci.*, **59**, 381-385 (1977)

NOTES

Zeta Potential and Surface Charge Components at Anatase/Electrolyte Interface

Zeta potential vs pH for the TiO_2 (anatase)/electrolyte system was measured for NaCl, CsCl, and NaI solutions of concentrations ranging from 0.0001 to 0.01 *M*. Surface ionization constants of anatase as well as $[SO^-]$ and $[SOH_2^+]$ concentrations vs pH were determined from electrokinetic data. Surface charge components were determined taking into account adsorption of background electrolyte ions and electrokinetic data for the system studied.

INTRODUCTION

To verify the ionization–complexation model of the electrical double layer at an oxide/electrolyte interface (1–4) a complete set of experimental data on adsorption of swamping electrolyte ions, potentiometric titration and electrokinetics is indispensable. The analysis for symmetrical 1:1 electrolytes is the simplest case, but because of their so-called "indifferency" there are not enough experimental adsorption data available in literature for these electrolytes. In the previous paper (5) potentiometric titration data and adsorption of background electrolyte ions results were presented for the TiO_2 (anatase)/electrolyte interface. The aim of this paper is to complete the above results with electrokinetic data for the same sample.

EXPERIMENTAL

The same sample of TiO_2 as described previously (5) has been used in the experiments. The electrophoretic mobility was determined using a Zeta-meter cylindrical electrophoresis cell. The electrokinetic potential was calculated from electrophoretic mobility data. The measurements were performed in NaCl, CsCl, and NaI solutions of concentrations ranging from 0.0001 to 0.01 *M*.

RESULTS AND DISCUSSION

Zeta potentials of TiO_2 as a function of pH and electrolyte concentration for NaI are depicted in Fig. 1. These data are representative of other electrolytes; the results differ only imperceptibly. The isoelectric point appears at pH 6 for all the electrolytes and pzc = iep (5).

Using the previously described double straight-line extrapolation method (6) the surface ionization constants defined in Eqs. [1] and [2] have been determined

$$pK_{a1}^{int} = pH - \log[SOH] + \log[SOH_2^+] + \frac{e\psi_0}{2.3kT}$$

$$= pQ_{a_1} + \frac{e\psi_0}{2.3kT} \qquad [1]$$

$$pK_{a2}^{int} = pH + \log[SOH] - \log[SO^-] + \frac{e\psi_0}{2.3kT}$$

$$= pQ_{a_2} + \frac{e\psi_0}{2.3kT}. \qquad [2]$$

This method is a modified version of that by James and Parks (4) since $pQ_{a1,a2}$ vs pH + $\sqrt{C}$ are plotted instead of $pQ_{a1,a2}$ vs $\alpha_\pm + \sqrt{C}$. Besides, electrokinetic instead of surface charge data are used to determine the $[SO^-]$ and $[SOH_2^+]$ components. Example data of the graphical determination of $pK_{a1,a2}^{int}$ are presented in Fig. 2. The constants determined in this way are $pK_{a1}^{int} = 3$, $pK_{a2}^{int} = 9$, and $\Delta pK_a = 6$ and are in good agreement with those obtained previously using the double extrapolation technique and potentiometric titration data (5).

Once $pK_{a1,a2}^{int}$ have been assessed from Eqs. [1] and [2] the surface potential vs pH relationships can be roughly estimated (6). The surface potential change per one pH unit far enough from the pzc (iep) is almost constant (about 56, 56, and 55 mV for 0.0001, 0.001, and 0.01 *M* solutions, respectively) and independent of electrolyte concentration. More accurate estimation of ψ_0–pH relationships in the vicinity of the isoelectric point is possible using the parabolic interpolation method (7).

In our previous paper (6) different "constants" were obtained for different ionic strengths. Because of this the double extrapolation was used to eliminate the electrolyte effect. In reality $pK_{a1,a2}^{int}$ constants are independent of electrolyte concentration and can be determined by two independent methods (4–6). The results obtained for the same sample are almost identical. Now, if $pK_{a1,a2}^{int}$ are known it seems justifiable to assume that all the curves $pQ_{a1,a2}$ vs pH have to meet at the same point $pK_{a1,a2}^{int}$. It means that these curves must bend in the vicinity of the pzc and therefore the $d\psi_0/d$pH characteristics are not straight lines. Surface potential vs pH characteristics obtained for anatase/NaI system by use of the parabolic interpolation method are depicted in Fig. 3. The detailed discussion on this subject is presented elsewhere (7).

In the ionization–complexation model of the electrical double layer the surface charge is defined as

0021-9797/86 $3.00

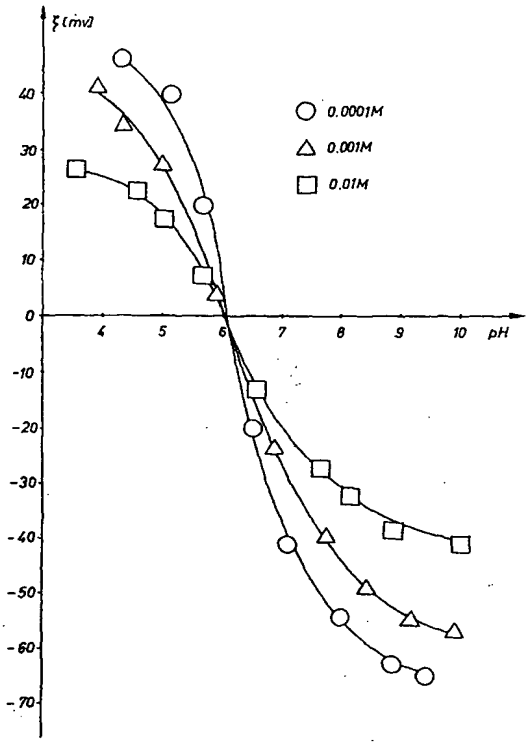

FIG. 1. Zeta potential of TiO_2 as a function of pH and NaI concentration.

$$\sigma_0 = B\{[SOH_2^+] + [SOH_2^+X^-] - [SO^-] - [SO^-Y^+]\}, \quad [3]$$

where

$$\sigma_\beta = B\{[SO^-Y^+] - [SOH_2^+X^-]\} \quad [4]$$

and

$$\sigma_d = B\{[SO^-] - [SOH_2^+]\}. \quad [5]$$

It is relatively easy to determine σ_β charge components from direct adsorption measurements of supporting electrolyte ions (5, 8). The same method, however, cannot be applied to estimate diffuse charge components because neither $[SO^-]$ nor $[SOH_2^+]$ can be determined by direct measurements. In this case an indirect method can be used.

Having estimated ψ_0–pH relationships and adsorption densities of cation and anion and knowing acidic and basic surface ionization constants it is possible to calculate the amounts of $[SO^-]$ and $[SOH_2^+]$ groups vs pH, in the whole pH range studied, taking into account Eqs. [1] and [2]. The concentrations of SOH groups is given by the expression (5)

$$[SOH] \cong N_s - [SO^-Y^+] - [SOH_2^+] - \frac{|\sigma_d|}{B}. \quad [6]$$

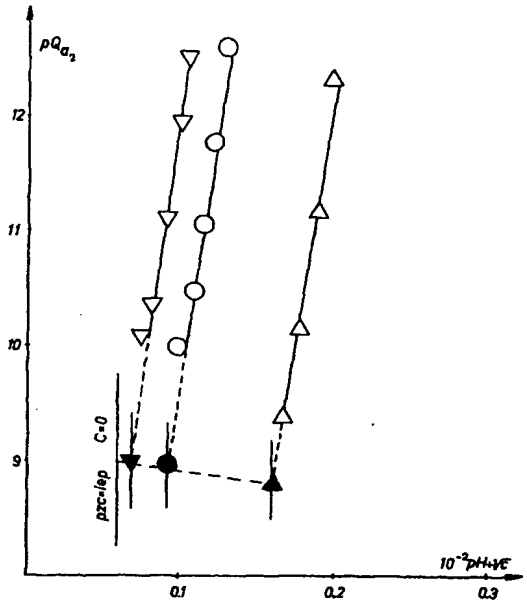

FIG. 2. Graphical determination of $pK_{\alpha 2}^{int}$ from electrokinetic data for TiO_2/NaI system.

As $[SO^-] \cong \sigma_d/B$ for $pH > pH_{pzc}$ and $[SOH_2^+] \cong -\sigma_d/B$ for $pH < pH_{pzc}$ (6), the lacking parts of $[SO^-]$ vs pH and $[SOH_2^+]$ vs pH should be determined for $pH < pH_{pzc}$ and $pH > pH_{pzc}$, respectively.

Using the ψ_0–pH characteristics for TiO_2 (see example data in Fig. 3) and adsorption data for the same sample (5), the amounts of $[SO^-]$ and $[SOH_2^+]$ groups vs pH of the solution have been calculated from Eqs. [1], [2], and [6]. For 0.0001 M solution, because adsorption densities

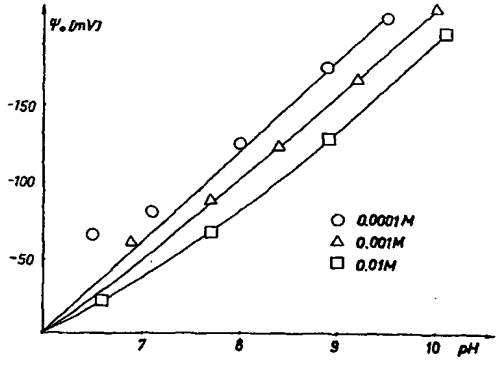

FIG. 3. Surface potential of anatase in NaI solutions vs pH for different electrolyte concentrations determined by use of curvilinear interpolation method (7).

and diffuse layer charges are very small in comparison with N_s, it is possible to assume simply that $[SOH] \cong N_s$ in the whole pH range studied. $N_s = 192\ \mu C \cdot cm^{-2}$ (expressed in charge units) has been assumed (2). The results obtained are presented in Fig. 4. The diffuse layer charges, σ_d, are also plotted for comparison.

As is clearly seen from Fig. 4, the diffuse charge curves almost coincide with $[SO^-]$ and $[SOH_2^+]$ curves for pH $>$ pH_{pzc} and pH $<$ pH_{pzc}, respectively, for 0.001 and 0.01 M solutions. The pH range where divergence between curves is observed, and the assumptions $\sigma_d \cong B[SO^-]$ or $\sigma_d \cong -B[SOH_2^+]$ are invalid (because the contributions of both groups are comparable) is about ±0.5 and ±1.0 pH units for 0.01 and 0.001 M solutions, respectively. For 0.0001 M solution this pH range is greater than ±2.0 units.

It is comprehensible because the derivative $d\sigma_d/d$pH increases as electrolyte concentration increases. Thus the pH range of the invalidity of the above assumptions expands as electrolyte concentration decreases.

These observations clearly show that the the hitherto existing assumptions that the contribution of $[SO^-]$ and $[SOH_2^+]$ groups for pH $<$ pH_{pzc} and pH $>$ pH_{pzc}, respectively, can be neglected (9, 10) is not throughout correct and depends on the electrolyte concentration.

All the curves in Fig. 4 show tendency to reach a "plateau" for extreme values of pH. This seems to be plausible and results from the below Equations. Equations [1] and [2] can be rewritten in the differential form as

$$1 + \frac{d \log \dfrac{[SOH_2^+]}{[SOH]}}{d\text{pH}} + \frac{e}{2.3kT}\frac{d\psi_0}{d\text{pH}} = 0 \qquad [7]$$

and

$$1 + \frac{d \log \dfrac{[SOH]}{[SO^-]}}{d\text{pH}} + \frac{e}{2.3kT}\frac{d\psi_0}{d\text{pH}} = 0. \qquad [8]$$

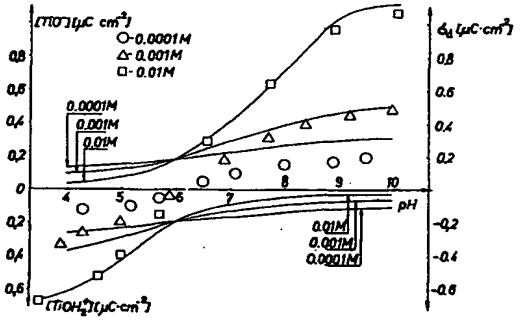

FIG. 4. Diffuse charge components for TiO_2/NaI system determined from electrokinetic data (solid lines). Net diffuse layer charges are presented for comparison (open symbols).

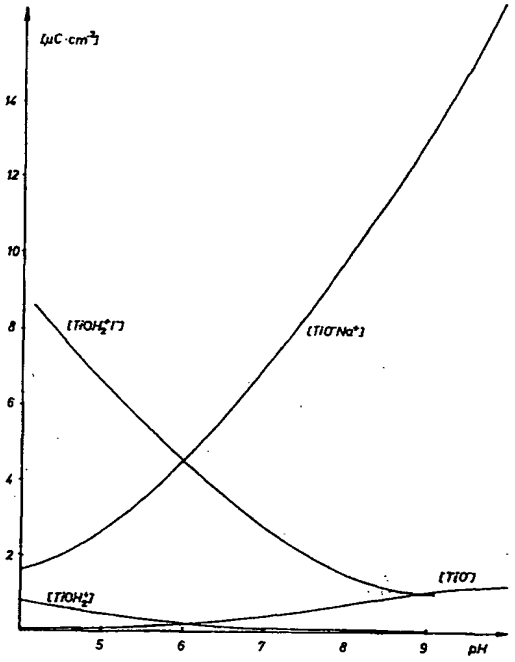

FIG. 5. Surface charge components for TiO_2/NaI system. Example data for 0.01 M solution.

It results from the data by Wiese *et al.* (11) that when ΔpH = pH − pH_{pzc} increases and electrolyte concentration decreases $d\psi_0/d$pH approaches −59.2 mV (see also Fig. 3 in this paper). Then the third terms in Eqs. [7] and [8] tend to −1 and the second terms in these equations approach zero. In other words far away from the pzc $[SOH_2^+]/[SOH]$ and $[SOH]/[SO^-]$ tend to a constant and therefore $[SOH_2^+]$ and $[SO^-]$ can reach a "plateau." The same phenomenon is observed experimentally for oxide/1:1 electrolyte systems where the ζ and/or σ_d vs pH curves tend to flatten off at extreme pH's (2, 8, 11, 12).

Taking into account the adsorption of swamping electrolyte ions (5) and the results described in this paper, the surface charge components have been determined for TiO_2. The example data for 0.01 M NaI solution are presented in Fig. 5. As is seen complexation reactions play a predominant part in surface charge creation. This was also observed by Regazzoni *et al.* for ZrO_2 and magnetite (12).

In the previous paper (5) to verify the ionization–complexation model of the electrical double layer, for 0.1 M electrolyte solutions the needed electrokinetic data for the described sample were determined by an extrapolation method on the basis of the results presented in this paper, because it was impossible to perform direct measurements of electrophoretic mobility in 0.1 M solutions. The results obtained for zeta potential are 10, 13, 17, and 19 mV for

pH values 7, 8, 9, and 10, respectively. The estimated potential drop was about 54 mV per one pH unit.

APPENDIX: NOMENCLATURE

B	conversion factor from mole·dm^{-3} to μC·cm^{-2} of charge
C	concentration of the electrolyte
e	electron charge
k	Boltzman constant
$K^{int}_{a1,a2}$	effective surface ionization constants
N_s	total number of surface sites available
$Q_{a1,a2}$	apparent ionization quotients
T	temperature
X^-, Y^+	anion and cation, respectively
$\alpha_\pm$	fraction of charged sites, σ_0/N_s
ψ_0, ψ_d	mean potential in the plane of surface charge, σ_0, and at the start of the diffuse layer, respectively
σ_0, σ_β, σ_d	net charge densities at the surface, in the plane of specifically adsorbed counterions, and diffuse layer, respectively
ζ	electrokinetic potential
iep	isoelectric point, $\sigma_d = 0$
pzc	point of zero surface charge, $\sigma_0 = 0$

ACKNOWLEDGMENT

The author would like to express his gratitude to the Polish Academy of Sciences, Institute of Catalysis and Surface Chemistry, Cracow, for financial support.

REFERENCES

1. Yates, D. E., Levine, S., and Healy, T. W., *J. Chem. Soc. Faraday Trans. 1* **70,** 1807 (1974).
2. Davis, J. A., James, R. O., and Leckie, J. O., *J. Colloid Interface Sci.* **63,** 480 (1978).
3. James, R. O., *in* "Adsorption of Inorganics at Solid/Liquid Interfaces" (M. A. Anderson and A. J. Rubin, Eds.), p. 219. Ann Arbor Science Pub., Ann Arbor, Mich., 1981.
4. James, R. O., and Parks, G. A., *in* "Surface and Colloid Science" (E. Matijevic, Ed.), Vol. 12, p. 119. Wiley–Interscience, New York, 1982.
5. Sprycha, R., *J. Colloid Interface Sci.* **102,** 173 (1984).
6. Sprycha, R., and Szczypa, J., *J. Colloid Interface Sci.* **102,** 288 (1984).
7. Sprycha, R., and Szczypa, J., *J. Colloid Interface Sci.*, in press.
8. Smit, W., and Holten, C. L. M., *J. Colloid Interface Sci.* **78,** 1 (1980).
9. Boehm, H. P., *Discuss. Faraday Soc.* **52,** 264 (1971).
10. Schindler, P. W., and Gamsjager, H., *Discuss. Faraday Soc.* **52,** 286 (1971).
11. Wiese, G. R., James, R. O., Yates, D. E., and Healy, T. W., *in* "International Review of Science" (J. O. M. Bockris, Ed.), Phys. Chem. Series 2, Vol. 6. Butterworths, London, 1976.
12. Regazzoni, A., Blesa, M. A., and Maroto, A. J. G., *J. Colloid Interface Sci.* **91,** 560 (1983).

RYSZARD SPRYCHA

Department of Radiochemistry and Colloid Chemistry
Institute of Chemistry
Maria Curie-Skłodowska University
Lublin, Poland

Received November 27, 1984